Acta Cryst E CRYSTALLOGRAPHIC COMMUNICATIONS

ISSN 2056-9890

Synthesis and crystal structure of silicon pernitride SiN_2 at 140 GPa

Pascal L. Jurzick,[a] Georg Krach,[b] Lukas Brüning,[a] Wolfgang Schnick[b] and Maxim Bykov[a]*

[a]Institute of Inorganic Chemistry, University of Cologne, Greinstrasse 6, 50939 Cologne, Germany, and [b]Department of Chemistry, University of Munich (LMU), Butenandtstrasse 5-13 (D), 81377 Munich, Germany. *Correspondence e-mail: maxim.bykov@uni-koeln.de

Received 17 August 2023
Accepted 14 September 2023

Edited by M. Weil, Vienna University of Technology, Austria

Keywords: nitrides; pernitrides; silicon nitrides; high pressure; crystal structure.

Supporting information: this article has supporting information at journals.iucr.org/e

Silicon pernitride, SiN_2, was synthesized from the elements at 140 GPa in a laser-heated diamond anvil cell. Its crystal structure was solved and refined by means of synchrotron-based single-crystal X-ray diffraction data. The title compound crystallizes in the pyrite structure type (space group $Pa\overline{3}$, No. 205). The Si atom occupies a site with multiplicity 4 (Wyckoff letter *b*, site symmetry .$\overline{3}$.), while the N atom is located on a site with multiplicity 8 (Wyckoff letter *c*, site symmetry .3.). The crystal structure of SiN_2 is comprised of slightly distorted [SiN_6] octahedra interconnected with each other by sharing vertices. Crystal chemical analysis of bond lengths suggests that Si has a formal oxidation state of +IV, while nitrogen forms pernitride anions $(N{-}N)^{4-}$.

1. Chemical context

Nitrogen-rich materials have gained a lot of attention due to their diverse properties such as high hardness, incompressibility (Young *et al.*, 2006; Bykov *et al.* 2019*a*) and high energy density (Bykov *et al.*, 2021; Wang *et al.*, 2022). Among these, binary high-pressure nitrides of group 14 elements are of particular interest, as they exhibit remarkable elastic and electronic properties compared to their ambient-pressure counterparts. In particular, cubic silicon nitride γ-Si_3N_4, synthesized from the elements at about 15 GPa, is significantly more incompressible than the ambient-pressure α- and β-polymorphs (Zerr *et al.*, 1999). Recently Niwa *et al.* (2017) have synthesized pernitrides of group 14 elements (SiN_2, SnN_2 and GeN_2) by using laser-heated diamond anvil cells at pressures above 60 GPa. The crystal structures of GeN_2 and SnN_2 were solved and refined against powder X-ray diffraction data. However, the weak X-ray powder pattern of SiN_2 only allowed the suggestion that SiN_2 crystallizes in the pyrite structure type, while no structure refinement was performed.

In this work, we synthesized SiN_2 from the elements at pressures of 140 GPa and examined it by means of synchrotron single-crystal X-ray diffraction in order to solve and refine its crystal structure.

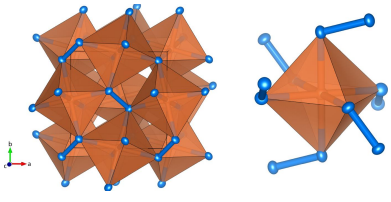

2. Structural commentary

SiN_2 crystallizes in fact in the pyrite structure type in the space group $Pa\overline{3}$ (No. 205). The asymmetric unit comprises two atoms, a silicon atom (multiplicity 4, Wyckoff letter *b*, site symmetry .$\overline{3}$.), and a nitrogen atom (8 *c*, .3.). The nitrogen atoms form N—N dimers, and consequently each of the N atoms is tetrahedrally coordinated by three Si atoms and one N atom. The centers of the N—N dimers form an *fcc* sublat-

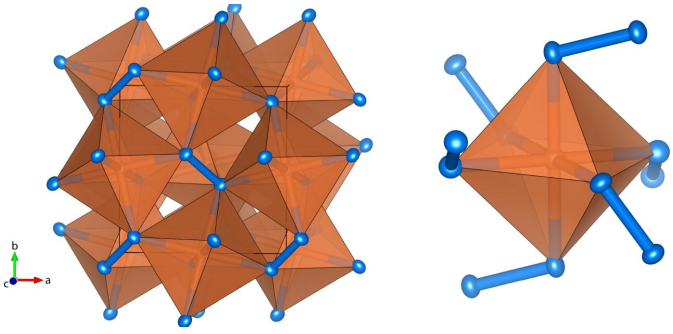

Figure 1
Crystal structure of SiN_2 at 140 GPa in polyhedral representation with Si atoms in orange and N atoms in blue. Shown are [SiN_6] octahedra interconnected by N atoms. Displacement ellipsoids are represented at the 75% probability level.

tice, which together with the interpenetrating *fcc* sublattice of Si atoms can be considered as a derivative of the rock salt structure type. Slightly distorted [SiN_6] octahedra [Si—N distance 6× 1.7517 (11) Å] interconnect with each other by sharing common vertices (Fig. 1). There is a linear correlation between the nitrogen–nitrogen distance in dimers and the formal ionic charge and bond order of the $(N_2)^{x-}$ anion (Laniel *et al.*, 2022). In the case of SiN_2, the refined nitrogen–nitrogen distance of 1.402 (8) Å indicates that the N—N bond has single-bond character. This distance is in a good agreement with N—N distances observed in other pernitrides that contain single-bonded $(N—N)^{4-}$ units (Tasnádi *et al.*, 2021). However, it is longer compared to N—N bonds in diazenides (Laniel *et al.*, 2022; Bykov *et al.*, 2020) and in dinitrides of trivalent metals (Niwa *et al.*, 2014; Bykov *et al.*, 2019*b*). Based on the empirical formula suggested by Laniel *et al.* (2022) for dinitrides, $FC = (BL - 1.104)/0.074$, where *FC* is the absolute value of the formal charge on the dinitrogen unit and *BL* is the N—N bond length in Å, a clear assignment can be made. For SiN_2, the value of FC was calculated as 4.04, which is in excellent agreement with the most common oxidation state of +IV for silicon.

3. Synthesis and crystallization

A piece of silicon (10×10×5 μm^3) was placed in the sample chamber of a BX90-type diamond anvil cell equipped with Boehler–Almax type diamonds using culets of 100 µm in diameter. The sample chamber was eventually created by laser-drilling a 50 µm hole in the Re gasket preindented to a thickness of 18 µm. Nitrogen, loaded using the high-pressure gas-loading system of the Bavarian Geoinstitute (Kurnosov *et al.*, 2008), served both as a pressure-transmitting medium and as a reagent. Pressure was determined by the shift of the diamond Raman band (Akahama & Kawamura, 2006). Upon compression to the target pressure of 140 GPa, the sample was heated using a focused Nd:YAG laser (λ = 1064 nm) to temperatures exceeding 2500 K. The heating duration was approximately 10 seconds. The reaction products consisted of multiple high-quality, single-crystalline domains.

Table 1
Experimental details.

Crystal data	
Chemical formula	SiN_2
M_r	56.11
Crystal system, space group	Cubic, $Pa\bar{3}$
Temperature (K)	293
a (Å)	4.1205 (5)
V (Å^3)	69.96 (3)
Z	4
Radiation type	Synchrotron, λ = 0.28457 Å
μ (mm^{-1})	0.21
Crystal size (mm)	0.001 × 0.001 × 0.001
Data collection	
Diffractometer	Customized ω-circle diffractometer
Absorption correction	Multi-scan (*CrysAlis PRO*; Rigaku OD, 2023)
T_{min}, T_{max}	0.750, 1.000
No. of measured, independent and observed [$I > 2\sigma(I)$] reflections	269, 101, 60
R_{int}	0.049
$(\sin\theta/\lambda)_{max}$ (Å^{-1})	1.112
Refinement	
$R[F^2 > 2\sigma(F^2)]$, $wR(F^2)$, S	0.071, 0.191, 1.07
No. of reflections	101
No. of parameters	6
$\Delta\rho_{max}$, $\Delta\rho_{min}$ (e Å^{-3})	1.08, −1.15

Computer programs: *CrysAlis PRO* (Rigaku OD, 2023), *SHELXT* (Sheldrick, 2015*a*), *SHELXL* (Sheldrick, 2015*b*), *VESTA* (Momma & Izumi, 2011) and *OLEX2* (Dolomanov *et al.*, 2009).

4. Refinement

Crystal data, data collection and structure refinement details are summarized in Table 1. The sample was studied by means of synchrotron single-crystal X-ray diffraction (SCXD) at the beamline ID11 (ESRF, Grenoble, France) with the following beamline setup: λ = 0.28457 Å, beamsize ∼0.7×0.7 μm^2, Eiger CdTe 2M detector. For the SCXD measurements, samples were rotated around a vertical ω-axis in the range ±30°. The diffraction images were acquired at an angular step $\Delta\omega = 0.5°$ and an exposure time of 5 s per frame. For analysis of the single-crystal diffraction data (indexing, data integration, frame scaling and absorption correction) we used the *CrysAlis PRO* software package (Rigaku OD, 2023). To calibrate an instrumental mode using *CrysAlis PRO*, *i.e.*, the sample-to-detector distance, detector origin, offsets of goniometer angles, and rotation of both X-ray beam and the detector around the instrument axis, we used a single crystal of orthoenstatite [$(Mg_{1.93}Fe_{0.06})(Si_{1.93},Al_{0.06})O_6$, space group *Pbca*, a = 8.8117 (2), b = 5.18320 (10), and c = 18.239 (13) Å].

Data analysis followed several steps:

1. After collecting SCXD data sets (series of ∼120 frames), a 3D peak search procedure was performed as implemented *CrysAlis PRO*. This search identified reflections from all crystalline phases present in the collection spot, including reaction products, initial reagents, pressure-transmitting medium, diamonds and gasket material.

2. The peak search table was processed by means of the *DaFi* program (Aslandukov *et al.*, 2022), which sorts reflections into groups: if reflections fall into one group they originate from one grain of the multigrain sample.

3. The reflection groups were assessed individually by indexing the reflections within the current group using built-in procedures in *CrysAlis PRO*. If indexing succeeded, the group was chosen for final data integration.

4. Datasets were integrated, and data was reduced following standard procedures, taking into account the shadowing of the diamond anvil cell.

Acknowledgements

We acknowledge the European Synchrotron Radiation Facility (ESRF) for provision of synchrotron radiation facilities and we would like to thank Pierre-Olivier Autran for assistance and support in using beamline ID11. We thank Dr Alexander Kurnosov for loading the DAC with nitrogen.

Funding information

Funding for this research was provided by: Deutsche Forschungsgemeinschaft (grant No. BY112/2-1 to Maxim Bykov). A PhD scholarship for GK from the Friedrich Naumann Foundation for Freedom with funds from the Federal Ministry of Education and Research (BMBF) is gratefully acknowledged.

References

Akahama, Y. & Kawamura, H. (2006). *J. Appl. Phys.* **100**, 043516.
Aslandukov, A., Aslandukov, M., Dubrovinskaia, N. & Dubrovinsky, L. (2022). *J. Appl. Cryst.* **55**, 1383–1391.
Bykov, M., Bykova, E., Ponomareva, A. V., Abrikosov, I. A., Chariton, S., Prakapenka, V. B., Mahmood, M. F., Dubrovinsky, L. & Goncharov, A. F. (2021). *Angew. Chem. Int. Ed.* **60**, 9003–9008.
Bykov, M., Chariton, S., Fei, H., Fedotenko, T., Aprilis, G., Ponomareva, A. V., Tasnádi, F., Abrikosov, I. A., Merle, B., Feldner, P., Vogel, S., Schnick, W., Prakapenka, V. B., Greenberg, E., Hanfland, M., Pakhomova, A., Liermann, H.-P., Katsura, T., Dubrovinskaia, N. & Dubrovinsky, L. (2019*a*). *Nat. Commun.* **10**, 2994.
Bykov, M., Tasca, K. R., Batyrev, I. G., Smith, D., Glazyrin, K., Chariton, S., Mahmood, M. & Goncharov, A. F. (2020). *Inorg. Chem.* **59**, 14819–14826.
Bykov, M., Yusenko, K. V., Bykova, E., Pakhomova, A., Kraus, W., Dubrovinskaia, N. & Dubrovinsky, L. (2019*b*). *Eur. J. Inorg. Chem.* pp. 3667–3671.
Dolomanov, O. V., Bourhis, L. J., Gildea, R. J., Howard, J. A. K. & Puschmann, H. (2009). *J. Appl. Cryst.* **42**, 339–341.
Kurnosov, A., Kantor, I., Boffa-Ballaran, T., Lindhardt, S., Dubrovinsky, L., Kuznetsov, A. & Zehnder, B. H. (2008). *Rev. Sci. Instrum.* **79**, 045110.
Laniel, D., Winkler, B., Fedotenko, T., Aslandukova, A., Aslandukov, A., Vogel, S., Meier, T., Bykov, M., Chariton, S., Glazyrin, K., Milman, V., Prakapenka, V., Schnick, W., Dubrovinsky, L. & Dubrovinskaia, N. (2022). *Phys. Rev. Mater.* **6**, 023402.
Momma, K. & Izumi, F. (2011). *J. Appl. Cryst.* **44**, 1272–1276.
Niwa, K., Ogasawara, H. & Hasegawa, M. (2017). *Dalton Trans.* **46**, 9750–9754.
Niwa, K., Suzuki, K., Muto, S., Tatsumi, K., Soda, K., Kikegawa, T. & Hasegawa, M. (2014). *Chem. A Eur. J.* **20**, 13885–13888.
Rigaku OD (2023). *CrysAlis PRO*. Rigaku Oxford Diffraction Corporation, Wroclaw, Poland.
Sheldrick, G. M. (2015*a*). *Acta Cryst.* A**71**, 3–8.
Sheldrick, G. M. (2015*b*). *Acta Cryst.* C**71**, 3–8.
Tasnádi, F., Bock, F., Ponomareva, A. V., Bykov, M., Khandarkhaeva, S., Dubrovinsky, L. & Abrikosov, I. A. (2021). *Phys. Rev. B*, **104**, 184103.
Wang, Y., Bykov, M., Chepkasov, I., Samtsevich, A., Bykova, E., Zhang, X., Jiang, S., Greenberg, E., Chariton, S., Prakapenka, V. B., Oganov, A. R. & Goncharov, A. F. (2022). *Nat. Chem.* **14**, 794–800.
Young, A. F., Sanloup, C., Gregoryanz, E., Scandolo, S., Hemley, R. J. & Mao, H. (2006). *Phys. Rev. Lett.* **96**, 155501.
Zerr, A., Miehe, G., Serghiou, G., Schwarz, M., Kroke, E., Riedel, R., Fuess, H., Kroll, P. & Boehler, R. (1999). *Nature*, **400**, 340–342.

supporting information

Acta Cryst. (2023). E**79**, 923-925 [https://doi.org/10.1107/S2056989023008058]

Synthesis and crystal structure of silicon pernitride SiN_2 at 140 GPa

Pascal L. Jurzick, Georg Krach, Lukas Brüning, Wolfgang Schnick and Maxim Bykov

Computing details

Data collection: *CrysAlis PRO* (Rigaku OD, 2023); cell refinement: *CrysAlis PRO* (Rigaku OD, 2023); data reduction: *CrysAlis PRO* (Rigaku OD, 2023); program(s) used to solve structure: *SHELXT* (Sheldrick, 2015*a*); program(s) used to refine structure: *SHELXL* (Sheldrick, 2015*b*); molecular graphics: *VESTA* (Momma & Izumi, 2011); software used to prepare material for publication: Olex2 (Dolomanov *et al.*, 2009).

Silicon pernitride

Crystal data

SiN_2
M_r = 56.11
Cubic, $Pa\overline{3}$
a = 4.1205 (5) Å
V = 69.96 (3) Å^3
Z = 4
$F(000)$ = 112
D_x = 5.327 Mg m^{-3}
Synchrotron radiation, λ = 0.28457 Å
Cell parameters from 79 reflections
θ = 3.4–16.4°
μ = 0.21 mm^{-1}
T = 293 K
Irregular, colourless
0.001 × 0.001 × 0.001 mm

Data collection

Customized ω-circle diffractometer
Radiation source: synchrotron, ESRF, beamline ID11
Synchrotron monochromator
Detector resolution: 5.0 pixels mm^{-1}
ω scans
Absorption correction: multi-scan (CrysAlisPro; Rigaku OD, 2023)
T_{min} = 0.750, T_{max} = 1.000
269 measured reflections
101 independent reflections
60 reflections with $I > 2\sigma(I)$
R_{int} = 0.049
θ_{max} = 18.5°, θ_{min} = 3.4°
h = −4→4
k = −7→8
l = −8→7

Refinement

Refinement on F^2
Least-squares matrix: full
$R[F^2 > 2\sigma(F^2)]$ = 0.071
$wR(F^2)$ = 0.191
S = 1.07
101 reflections
6 parameters
0 restraints
Primary atom site location: dual
$w = 1/[\sigma^2(F_o^2) + (0.109P)^2]$ where $P = (F_o^2 + 2F_c^2)/3$
$(\Delta/\sigma)_{max} < 0.001$
$\Delta\rho_{max}$ = 1.08 e Å^{-3}
$\Delta\rho_{min}$ = −1.15 e Å^{-3}

Special details

Geometry. All esds (except the esd in the dihedral angle between two l.s. planes) are estimated using the full covariance matrix. The cell esds are taken into account individually in the estimation of esds in distances, angles and torsion angles; correlations between esds in cell parameters are only used when they are defined by crystal symmetry. An approximate (isotropic) treatment of cell esds is used for estimating esds involving l.s. planes.

Fractional atomic coordinates and isotropic or equivalent isotropic displacement parameters (Å²)

	x	*y*	*z*	U_{iso}*/U_{eq}
Si1	0.5000	0.5000	0.5000	0.0084 (5)
N1	0.5982 (5)	0.4018 (5)	0.9018 (5)	0.0076 (6)

Atomic displacement parameters (Å²)

	U^{11}	U^{22}	U^{33}	U^{12}	U^{13}	U^{23}
Si1	0.0084 (5)	0.0084 (5)	0.0084 (5)	−0.0005 (3)	−0.0005 (3)	−0.0005 (3)
N1	0.0076 (6)	0.0076 (6)	0.0076 (6)	0.0012 (8)	0.0012 (8)	−0.0012 (8)

Geometric parameters (Å, º)

Si1—N1	1.7517 (11)	Si1—N1^{v}	1.7517 (11)
Si1—N1^{i}	1.7517 (11)	N1—Si1^{vi}	1.7517 (11)
Si1—N1^{ii}	1.7517 (11)	N1—Si1^{vii}	1.7517 (11)
Si1—N1^{iii}	1.7517 (11)	N1—N1^{viii}	1.402 (8)
Si1—N1^{iv}	1.7517 (11)		
N1—Si1—N1^{iii}	86.94 (4)	N1^{iv}—Si1—N1^{ii}	86.94 (4)
N1^{iv}—Si1—N1^{v}	93.06 (4)	N1^{v}—Si1—N1^{i}	86.94 (4)
N1^{ii}—Si1—N1^{i}	93.06 (4)	N1—Si1—N1^{v}	86.94 (4)
N1—Si1—N1^{iv}	180.0	N1—Si1—N1^{i}	93.06 (4)
N1^{iii}—Si1—N1^{i}	180.00 (14)	Si1—N1—Si1^{vi}	112.54 (10)
N1^{iii}—Si1—N1^{iv}	93.06 (4)	Si1^{vii}—N1—Si1^{vi}	112.54 (10)
N1^{iii}—Si1—N1^{v}	93.06 (4)	Si1^{vii}—N1—Si1	112.54 (10)
N1—Si1—N1^{ii}	93.06 (4)	N1^{viii}—N1—Si1^{vi}	106.20 (12)
N1^{ii}—Si1—N1^{v}	180.0	N1^{viii}—N1—Si1^{vii}	106.20 (12)
N1^{iii}—Si1—N1^{ii}	86.94 (4)	N1^{viii}—N1—Si1	106.20 (12)
N1^{iv}—Si1—N1^{i}	86.94 (4)		
N1^{iii}—Si1—N1—Si1^{vii}	94.59 (6)	N1^{i}—Si1—N1—Si1^{vii}	−85.41 (6)
N1^{iii}—Si1—N1—Si1^{vi}	−33.8 (3)	N1^{ii}—Si1—N1—Si1^{vii}	7.82 (11)
N1^{v}—Si1—N1—Si1^{vi}	59.4 (2)	N1^{iii}—Si1—N1—N1^{viii}	−149.62 (10)
N1^{i}—Si1—N1—Si1^{vi}	146.2 (3)	N1^{v}—Si1—N1—N1^{viii}	−56.39 (6)
N1^{ii}—Si1—N1—Si1^{vi}	−120.6 (2)	N1^{i}—Si1—N1—N1^{viii}	30.38 (10)
N1^{v}—Si1—N1—Si1^{vii}	−172.18 (11)	N1^{ii}—Si1—N1—N1^{viii}	123.61 (6)

Symmetry codes: (i) −*x*+1, *y*+1/2, −*z*+3/2; (ii) −*x*+3/2, −*y*+1, *z*−1/2; (iii) *x*, −*y*+1/2, *z*−1/2; (iv) −*x*+1, −*y*+1, −*z*+1; (v) *x*−1/2, *y*, −*z*+3/2; (vi) −*x*+1, *y*−1/2, −*z*+3/2; (vii) −*x*+3/2, −*y*+1, *z*+1/2; (viii) −*x*+1, −*y*+1, −*z*+2.